Test of the Weak-Coupling Triaxial Model for ^{143}Eu

A. Aryaeinejad, R.B. Firestone, W.H. Bentley and W.C. McHarris

A total of 31 states in ^{143}Eu, some of which have not been seen in β-decay, were observed in an in-beam experiment, (see the level scheme in this annual report). These states can be classified into three different categories: 1) Single-quasiparticle states, 2) Negative-parity collective states, and 3) Positive-parity collective states.

Single-Particle States

The four levels at 0, 271.9, 389.5 and 463.0 keV can be described as $\pi d5/2$, $\pi g7/2$, $\pi h11/2$, and $\pi s1/2$ single-quasiparticle shell model states respectively. These four states in the N=82 isotones have been successfully analyzed by de Takacsy and Das Gupta[1] as single-quasiparticle states. It is important here to mention that the level at 258.8 keV with $J^\pi = 3/2^+$ is probably not a $\pi d3/2$ single-quasiparticle state. The $\pi d3/2$ single-quasiparticle state, in the case of other N=80 odd-mass isotones, lies above 400 keV; therefore it is unlikely to see this state at such low energy in ^{143}Eu. On the other hand, our calculation (which will be discussed later) shows that the 258.8 keV state is the coupled state of d5/2 plus ^{142}Sm core.

Negative-Parity Collective States

The negative-parity collective states in ^{143}Eu are expected to be built mainly on the h11/2 proton level using a triaxial weak-coupling model described by Meyerter-Vehn.[2] The lowest excited states of the ^{142}Sm adjacent even nucleus has been used in order to find deformation parameter and the asymmetry parameter. Since the triaxial model applied to the even-even neighbours does not distinguish between prolate deformation $0^\circ < \gamma < 30^\circ$ and oblate deformation $30^\circ < \gamma < 60^\circ$, both prolate and oblate deformations were considered. The results are shown in figure 1.

For prolate shape (γ=23.5°), the agreement with the experiment is not good, neither in the level ordering nor the energy separation. The calculated energy of the second $11/2^-$ state (1897.0 keV), first $9/2^-$ state (1186.0 keV) and the first $13/2^-$ state (1508.0 keV) are much greater than the experiment. The prolate calculations place the first $7/2^-$ state at 979.0 keV which has not been observed experimentally. In fact, on prolate-oblate shape transition between N=77 and N=79 neodymium isotopes has been reported by J. Gizon et al.,[3] and we might expect ^{143}Eu (N=80) to be oblate.

For the oblate deformation, negative parity-states were calculated both for γ=36.5° (60°-23.5°) and γ=60°. The agreement with the experiment is much improved, both in the level ordering and energy separation of the lower states, with the exception of the first $15/2^-$ state. The calculated energy levels of the first $9/2^-$ (900.0 keV), first $13/2^-$ (1058.0 keV), first $15/2^-$ (1365.0 keV), second $11/2^-$ (1386.0 keV), first $7/2^-$ (1472.0 keV) and the first $19/2^-$ (2655.0 keV) for γ=36.5° confirm an oblate-type shape for ^{143}Eu. Evidence for triaxiality are generally the second and third $11/2^-$ (1386.0 and 2295.0 keV, respectively) as well as the second and third $9/2^-$ (2220.0 and 2506.0 keV, respectively) which have been observed in the experiment. Thus the higher states favor or triaxial description in preference to a pure oblate shape.

Positive-Parity Collective States

The positive-parity collective states are generated from the d5/2 and g7/2 proton state. Here the couplings give poor results due to mixing with neighboring shells of the same parity. Figure 2 shows the results of coupling d5/2 and g7/2 proton state with a ^{142}Sm core for γ=36.5°.

The ($\pi d5/2$ + core) couplings lead to the level $3/2^+$ at 253.0 keV which were observed in the experiment at 258.8 keV. This indicates that the 258.8 keV state is not a single-quasiparticle state but rather a collective state. In fact, the $3/2^+$ single-quasiparticle state has been observed at 405.0 and 403.9 keV in ^{139}Pr and ^{143}Pm, respectively. For the other N=80 odd-mass isotones, this state lies at a higher excitation.

The calculated $1/2^+$ state for the d5/2 system at 789.0 keV might be either the 803.5 keV state in in-beam work with no spin assignment or the 812.9 keV state in β-decay work.[4] According to d5/2 system calculations, the first $3/2^+$ state and second $1/2^+$ state lie at 1546.0 keV and 1929.0 keV, respectively. These states have not been observed in-beam, but from β-decay work they are placed at 1543.0 keV and 1723.6 keV, respectively.

The (g7/2 + core) couplings place the first $11/2^+$ state at 1061.0 keV. Indeed, this level has been observed experimentally at 1057.5 keV.

Finally, the level at 907.1 keV with the spin of $9/2^+$ can be seen theoretically at 732.0 keV in $d5/2^-$ system and at 950 keV in $g7/2^-$ system. The fact that this level feeds directly to ground state and not to 271.9 keV state leads us to believe this state is d5/2 single-proton state coupled to the first 2^+ state in ^{142}Sm.

For the high-lying positive-parity states, it is difficult to predict which states are composed of which principal components; first because of lack of information about definite spin assignments, and secondly, because they may mix strongly with nearby states.

The triaxial weak-coupling model seems to be a good model to describe the level structure in ^{143}Eu. The calculations for negative-parity collective states indicate that ^{143}Eu has an oblate shape. Some of the low-lying positive-parity collective states were also reproduced.

---

1. N. de Takacsy and S. Das Guptor, Phys. Rev. C 13, 399 (1976).
2. J. Meyerter-Vehn, Nucl. Phys. A249, 111 (1975).
3. J. Gizon, A. Gizon, R.M. Diamond and F.S. Stephen and F.S. Stephen, J. Phys. G. Nucl. Phys. Vol. 4, No. 7 L171 (1978).
4. R.B. Firestone, R.A. Warner, Wm. C. McHarris and W.H. Kelly, Phys. Rev. C 17, 718 (1978).

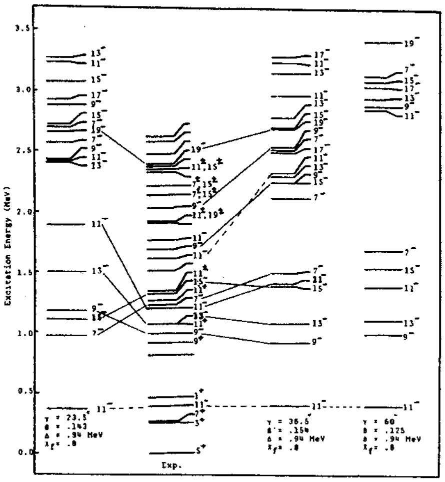

Fig. 1. Experimental and theoretical excitation energy in ^{143}Eu. The theoretical values are calculated for negative-parity collective states by using triaxial weak-coupling model. Spins are shown in units of 2J.

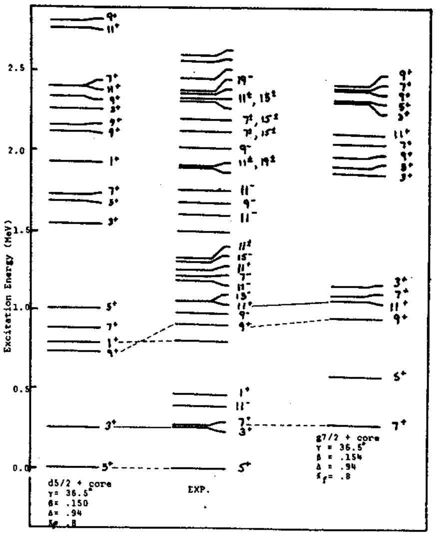

Fig. 2. Experimental and theoretical excitation energy in ^{143}Eu. The theoreical values are calculated for positive-parity collective states by using triaxial weak-coupling model. Spins are shown in units of 2J.

Sidebands in ^{168}Yb Studied by the (α,2n) Reaction

J.L.S. Carvalho, P.M. Walker, W.H. Bentley, and S.R. Faber

Much work has been done on prolate nuclei in the region A = 160-180 where the rotational ground state bands have been well established, to a reasonably high spin, for many years. Many of the deformed even-even nuclei of the rare-earths in this region display interesting behavior like low-lying negative-parity bands that seem to be based on either aligned two quasi-particle configurations ($A \simeq 160$) or single-phonon octupole vibrations ($A \simeq 180$).

Another interesting effect in this region is the backbending anomaly which affects almost all rare-earths. This effect is seen at the N = 96 and 100 isotones, but the even-even N = 98 isotones do not show such anomaly in their yrast bands.

The N = 98 isotone, ^{168}Yb, is being studied to help understand such phenomena. Since the feeding patterns of the nuclear levels are related to the distribution of angular momentum brought in by the projectile, light projectiles would seem ideal for studying the lower spins of the side bands. The (HI,xn) reactions can be used then to obtain information about the higher levels of rotational and vibrational bands in these deformed nuclei.

An oxide target of ^{166}Er was bombarded with 27 MeV alpha particles, produced by the MSU cyclotron, in order to obtain ^{168}Yb. The experiments performed included γ-γ-t coincidence and γ-angular distributions.

In the coincidence experiment one high purity, high resolution Ge detector and a Ge(Li) detector were placed at 90° with respect to the beam direction. Three parameters were set (energy$_1$-energy$_2$-time) and the data were stored event-by-event on magnetic tapes. By using computer programs the events were sorted out into gated coincidence spectra.

The γ-ray angular distribution experiment was performed with two Ge(Li) detectors mounted on the MSU goniometer apparatus at six different angles (between 90°-160° with respect to the beam). One of the Ge(Li) detectors was used as a monitor detector in order to perform intensity normalizations between angles. From the peak intensities at each energy, Legendre Polynomials can be fitted and the resulting A_2 and A_4 coefficients can be compared to theoretical values to determine the probable transition multipolarities.

Using the data from the coincidence experiment we were able to determine a preliminary decay scheme, with the gsb up to 14 $\hbar$ as well as several vibrational bands (up to about 11 $\hbar$). A precise energy calibration is being done currently with the computer program SAMPO since several doublets were found in the coincidence spectra, greatly complicating the sorting out of the level transitions.

---

1. R. Graetzer et al., Nucl. Phys. 76, 1 (1966).

Sidebands in ^{170}Yb Studied by (α,2n) and (α,4n) Reactions

P.M. Walker, S.R. Faber, W.H. Bentley, R.M. Ronningen, R.B. Firestone, and F.M. Bernthal

The systematic variations in the properties of the negative-parity yrast bands in deformed even-even nuclei gives insight into the effects of the quaisparticle structure on the rational behaviour. The N = 100 isotones cover a range of properties: ^{168}Er has[1] a strongly-coupled $K = 4^-$ band with an isomeric bandhead, while ^{172}Hf and ^{174}W have[2,3] decoupled negative-parity yrast bands with no obvious bandheads.

We have undertaken a detailed investigation of the intermediate isotone, ^{170}Yb, using both the (α,2n) and the (α,4n) reactions, at 27 MeV and 50 MeV respectively. Beams were provided by the MSU cyclotron. Three parameter γ-γ-time event-by-event recordings were used to establish the level scheme and obtain lifetime information. Short half-lives ($0.5 < t_{1/2} < 20$ ns) were measured with two-parameter γ-time (beam timing) event-by-event recording. Spins were obtained from angular distributions, and parities from electron conversion measurements.

A partial level scheme is shown in the figure, illustrating levels in both the positive-parity and the negative-parity yrast bands. Three other sidebands have been identified, one with a bandhead at 2190 keV and a half-life of 2.8 ns. The negative-parity yrast band (see figure) has unusual properties in that the isomeric I = 4 bandhead is characteristic of a strongly-coupled K = 4 band (i.e. similar to ^{168}Er), while the decays of the odd-spin members promptly ($t_{1/2} < 0.5$ ns) to the ground-state band implies a lower K-value, and is similar to the behaviour in the isotones ^{172}Hf and ^{174}W. Furthermore, the band has a high moment of inertia, characteristic of rotational alignment. The angular distribution measurements for the in-band $I \rightarrow I - 1$ transitions enable us to make the $\{7/2^+[633]_n, 5/2^-[512]_n\}_{4^-}$ two-quasineutron singlet assignment, though there is also evidence for mixing with lower-K states. These properties may be understood[4] as a consequence of the involvement of the $7/2^+[633]$, $i_{13/2}$ neutron, whose high j leads to strong Coriolis effects. The gradual structural changes from ^{168}Er to ^{174}W, i.e. from strong coupling to decoupling in the negative-parity yrast bands, would appear to be consistent with the effects of larger hexadecapole deformations in the heavier isotones. This would lead to reduced energy separation between the $i_{13/2}$ orbitals and hence to greater mixing between them.

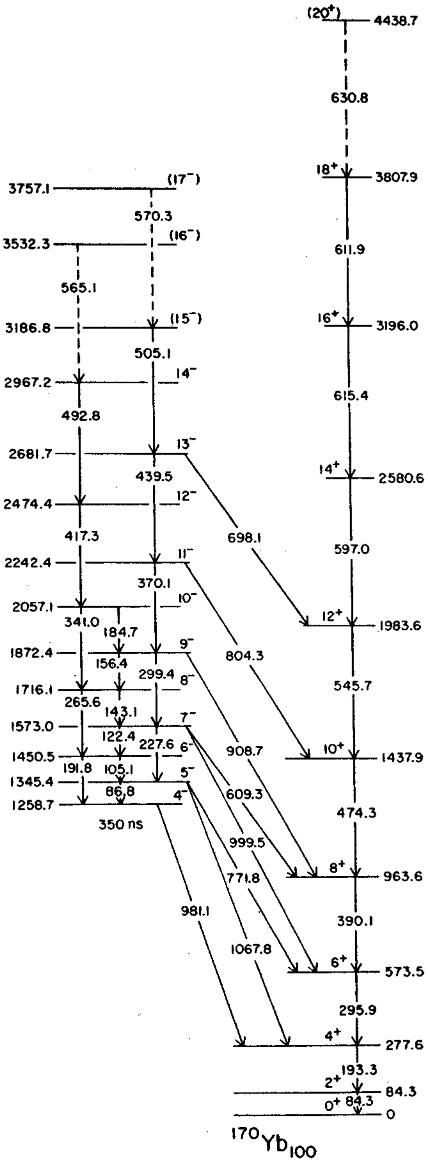

---

1. H.R. Koch, A. Phys. 192, 142 (1966).
2. P.M. Walker, G.D. Dracoulis, A. Johnson, and J.R. Leigh, Nucl. Phys. A293, 481 (1977).
3. G.D. Dracoulis, P.M. Walker, and A. Johnston, J. Phys. G. (Nucl. Phys.) 4, 713 (1978).
4. P.M. Walker, S.R. Faber, W.H. Bentley, R.M. Ronningen, R.B. Firestone, and F.M. Bernthal, Phys. Lett. B, in press.

Sidebands in ^{172}Yb Studied by the (α,2n) Reaction

P.M. Walker, S.R. Faber, W.H. Bentley, R.M. Ronningen and R.B. Firestone

The sideband structure in deformed even-even nuclei gives detailed information on the competition between rotational, vibrational and quasiparticle degrees of freedom. The role of the $i_{13/2}$ neutrons in the rare-earth region is of special interest due to the influence of Coriolis forces, and the relevance to backbending phenomena. Opposite couplings of a $7/2^+$[633], $i_{13/2}$ neutron with a $5/2^-$[512] neutron, forming $K=1^-$ and 6^- bands, are already known in ^{172}Yb from particle transfer[1] and other studies.

We have undertaken a detailed investigation of ^{172}Yb using the (α,2n) reaction at 27 MeV, with beams from the MSU Cyclotron, and are able to identify states up to spin 14 in these sidebands. Three other sidebands are also populated. The techniques used include γ-γ-time and γ-time (beam timing) event-by-event recording, electron conversion measurements and angular distributions.

The $K=1^-$ band is known[2] to have collective properties characteristic of the single-phonon octupole vibration. The band is decoupled into odd-spin and even-spin sequences, the odd spins being favoured energetically, which can be understood from mixing with the $K=0^-$ octupole band. Alternatively, Coriolis effects on the high-j, $7/2^+$[633] neutron may explain the band properties.

In the figure we have shown how the total angular momentum, I, varies with the rotational frequency, $\hbar w$, and following ref. 3 we observe that at high rotational frequency the angular momentum aligned with the rotation, i_α, is about 3.5 $\hbar$ in the odd-spin sequence of the 1^- band. This is more than can be obtained from alignment of the octupole angular momentum ($3\hbar$) and may be interpreted as evidence for alignment of individual particle angular momenta, presumably mainly from the $i_{13/2}$ neutron. Values for the 6^- band are also shown in the figure, and similar alignment is evident. Although the $7/2^+$[633] and $5/2^-$[512] neutrons have opposite couplings in the two bands, it appears as though the $i_{13/2}$ neutron aligns with the rotation independently of this coupling.

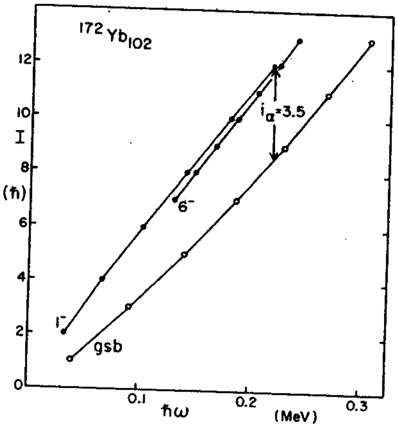

Fig. 1.

---

[1] R.A. O'Neil and D.G. Burke, Nucl. Phys. A182, 342 (1972).

[2] D.G. Burke and B. Elbek, Dan Mat. Fys. Medd 36, No. 6 (1967).

[3] A. Bohr and B.R. Mottelson, Proc. Int. Conf. Nucl. Structure, Tokyo 1977, J. Phys. Soc. Japan 44, Suppl. 157 (1978).

Excited States in ^{141}Pm Via the $(P,2n\gamma)$ and $(\alpha,4n\gamma)$ Reactions

R. Araeinejad, R.B. Firestone, B.H. Bentley and Wm. C. McHarris

A series of investigations of the N=80 odd mass nuclei are underway to study the excited states in these nuclei (^{143}Eu, ^{141}Pm and ^{139}Pr) populated via in-beam techniques and to see if a triaxial model is a good model to explain resulting level structure.[1]

Levels in ^{141}Pm were populated by the $(P,2n\gamma)$ and $(\alpha,4n\gamma)$ reactions. The experiments include gamma-ray singles, coincidence and angular distributions measurements. In all of these experiments high resolution Ge(Li) detectors were used.

Shown in Fig. 1 and Fig. 2 are tentative decay schemes for $(P,2n\gamma)$ and $(\alpha,4n\gamma)$ respectively, which are the results of a preliminary analysis of data. The analysis of angular distributions measurements are still in progress in order to complete level schemes.

The 628.6 keV isomeric state in ^{141}Pm de excites to the ground state primarily via a state at 196.6 keV with the emmission of 431.8 and 196.6 keV γ-rays. The half-life of this state was measured to be 0.22 ± .01 μs by Arl't et al.,[2] 0.70 ± 0.22 μs by Warner et al.[3] and 0.59 ± 0.02 μs by Kennedy et al.[4] From our coincidences experiment for $(\gamma,4n\alpha)$ reaction we were able to measure the half-life of this state. We used a fast-slow coincidence system with two Ge(Li) detectors and a time to amplitude converter (TAC). The coincidence timing resolution was 4.0 μs. The x-axis was gated on the 431.8 keV transition and the y-axis was gated on the entire spectrum above 450 keV. The time spectrum is shown in Fig. 3. After background subtractions, and using the computer code KINFIT, the half-life for the 628.6 keV state turned out to be .627 ± .023 μs.

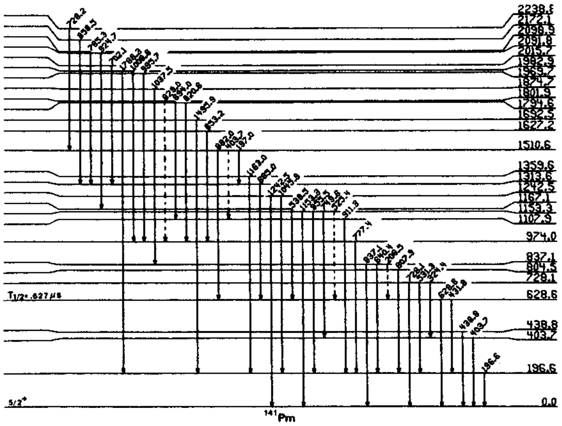

Fig. 1. The tentative level scheme of ^{141}Pm obtained from the $(P,2n\gamma)$ data.

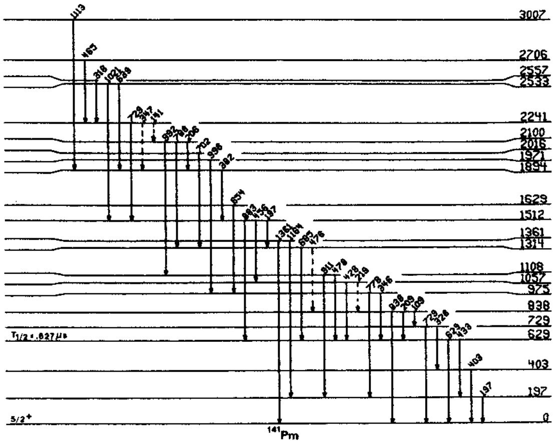

Fig. 2. The tentative level scheme of ^{141}Pm obtained from the $(\alpha,4n\gamma)$ data.

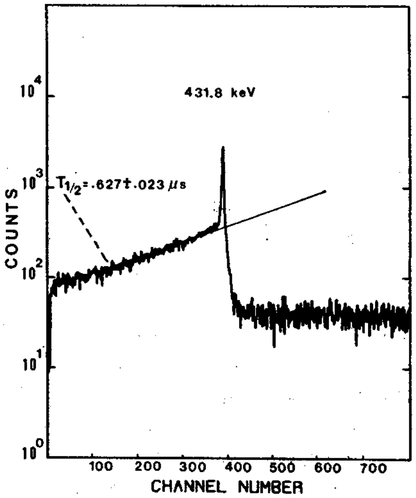

Fig. 3. Time axis projection on an semi-logarithmic plot illustrating the half-life of 431.8 keV transitions in ^{141}Pm.

---

1. See the articles regarding ^{143}Eu in this report.
2. R. Arl't., G. Beyer, Y. Vanryschuk, V.A. Morosov, T.M. Muminov, V.I. Rason, J. Sazynski, H. Faia, H. Strusny and E. Herrmann, JINR Report No. P6-5517, 1970 (unpublished).
3. R.A. Warner, R.R. Todd, R.E. Eppley, W.H. Kelly and Wm. C. McHarris, Bull. Am. Phys. Soc. 16, 1161 (1971).
4. G.G. Kennedy, J. Deslavriers, S.C. Gujrathi and S.K. Mark, Phys. Rev. C 15, No. 2 (1977).

In-Beam γ-Ray Spectroscopy of Excited States In ^{143}Eu

R. Aryaeinejad, R.B. Firestone, W.H. Bentley and W.C. McHarris

One of the most interesting regions of the nuclidic chart for current study is the region just below N=82 closed shell. The neutron deficient of N=80 odd-mass isotones located in this region are transitional nuclei between spherical and strongly deformed nuclear shapes. For many of these nuclei, weak-coupling features of the level scheme are expected and one can hope that the trixial model will be a good model for explaining these nuclei.

The level shcemes of ^{143}Eu in this region has been previously investigated by β-decay. We report the results of an in-beam study using (P,2nγ) reaction on levels in ^{143}Eu. Many experiments such as γ-γ coincidence, excitation functions and angular distributions were carried out.

^{143}Eu singles spectron was taken with a 10% efficient Ge(Li) detector (with resolution 2.4 keV FWHM at 1332 keV) at 125° in order to minimize angular distribution effects.

The Code ALLICE[1] was run to determine the optimal energy for the (p,2nγ) reaction, and spectra were taken at 30, 35 and 40 MeV proton energies to study the excitation function of the transitrons in ^{143}Eu. Figure 1 shows the excitation functions for some γ-rays in ^{143}Eu γ-ray intensities were normalized with respect to 271.9 keV γ-ray, then relative intensities for each γ-ray at different beam energies were obtained relative to 30 MeV intensities. Many γ-rays from competing reactions were recognized easily in this manner.

γ-γ coincidence data taken using two Ge(Li) detectors with the addresses of the coincident events being stored serially on magnetic tape for off-line analysis of a later time. The coincidence information and energy summing relationships were used to construct a level scheme. The data from the angular distributions, excitation functions and singles spectra were then used to lend support to the scheme. Figure 2 shows a level scheme of ^{143}Eu. A total of 37 γ-rays deexciting 31 states were assigned from the result of this experiment.

Spin assignments were made to some of these levels based on the results of the angular distribution experiment and experimental electron connersion coefficients taken from Wisshak et al.[2] A γ-ray angular distribution measurements were made in random order at angles of 90°, 100°, 110°, 125°, 140° and 155°. Isotropic transitions 271.9 and 117.5 keV in ^{143}Eu were used as an internal normalization for the angular distributions. The data were fit to equations;

$$W(\theta) = 1 + A_2 P_2(\cos\theta) + A_4 P_4(\cos\theta)$$

using the computer code Gadfit[3] to obtain experimental A_2 and A_4 values. In Fig. 2 those spins indicated by an asterisk are taken from β-decay work.[4]

---

[1] M. Blann and F. Plasil, and unpublished nuclear enaporation code.

[2] K. Wisshak, A. Hanser, H. Kleure-Neclenius, J. Buchmann, H. Rebel, H. Faust, H. Toke and A. Fassler, Z. Phys. A 277, 129 (1976).

[3] Badfit, computer code written by R.A. Warner, MSU Cyclotron Lab. (unpublished).

[4] R.B. Firestone, R.A. Warner, Wm. C. McHarris and W.H. Kelly Phy. Rev. C 17, 718 (1978).

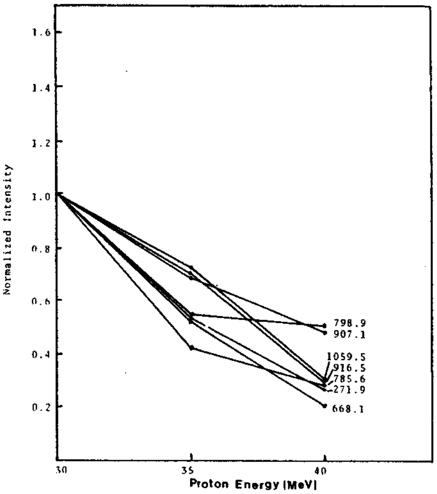

Fig. 1. Excitation functions of some γ-rays in ^{143}Eu.

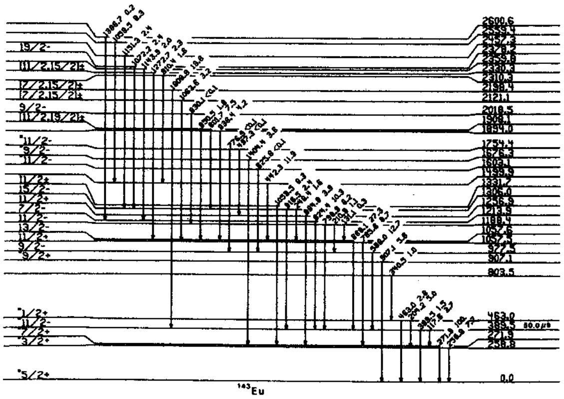

Fig. 2. The level scheme of ^{143}Eu obtained from the (p,2nγ) data.

High Spin States in ^{116}Sb

W.H. Bentley, C.B. Morgan, W.H. Kelly, and Wm. C. McHarris

As a continuation of the ongoing study of Sb nuclei, experiments were performed to excite the high spin states in ^{116}Sb. The reaction used in this study was the (α,3nγ) reaction. The experiments performed included γ-γ coincidence, angular distributions and half life measurements. In addition conversion coefficient measurements were recently performed and are presently being analyzed. The target used for all of these experiments was a natural Indium foil.

Preliminary results of these experiments were given in a previous annual report.[1] A more complete analysis of the data has resulted in the level scheme shown in Fig. 1. All of the levels shown decay through the J=8$^-$ isomer, whose absolute excitation energy is not accurately known. Consequently the excitation energies of all the levels shown are not accurately known. An approximate determination of 225 ± 60 keV has been made by R. Kamermans et al.[2] for this level. This is the value which is used in Fig. 1. Also note the spin assignments for all of the levels are based on the known 8$^-$ spin of this isomeric level.[3]

A comparison of the ^{116}Sb level scheme shown here with that of the high spin level structure of ^{115,117}Sb,[4] reveals several striking similarities. As in the neighboring odd-mass nuclei, the decay of high spin levels in ^{116}Sb proceeds through two separate sequences of γ-rays. The decay sequence drawn on the left in Fig. 1 carries more than half the intensity going into the 8$^-$ isomer. The energies, angular distributions, and relative intensities of the lower lying γ-rays in this sequence are very similar to the corresponding sequence in the neighboring odd-mass nuclei. This observation indicates that these lower lying levels can be characterized as the corresponding levels in the neighboring odd-mass nuclei coupled to maximum spin with an h 11/2 neutron state.

The remaining decay sequence shown on the right in Fig. 1 displays two rotational bands. This again is very similar to the neighboring odd-mass case, where a rotational band built on a g 9/2 proton hole state has been observed. The rotational bands in ^{116}Sb are very likely this same proton state coupled to a high spin neutron state. The available neutron states satisfying the necessary conditions are the g 7/2 and h 11/2 single particle orbitals. A determination of the parity of the band heads would distinguish between these two possibilities. It is hoped that the results of the recently performed conversion electron experiment will allow such a determination to be made. Alternative explanations of these rotational bands would involve much more complex structures, such as four quasi-particle states.

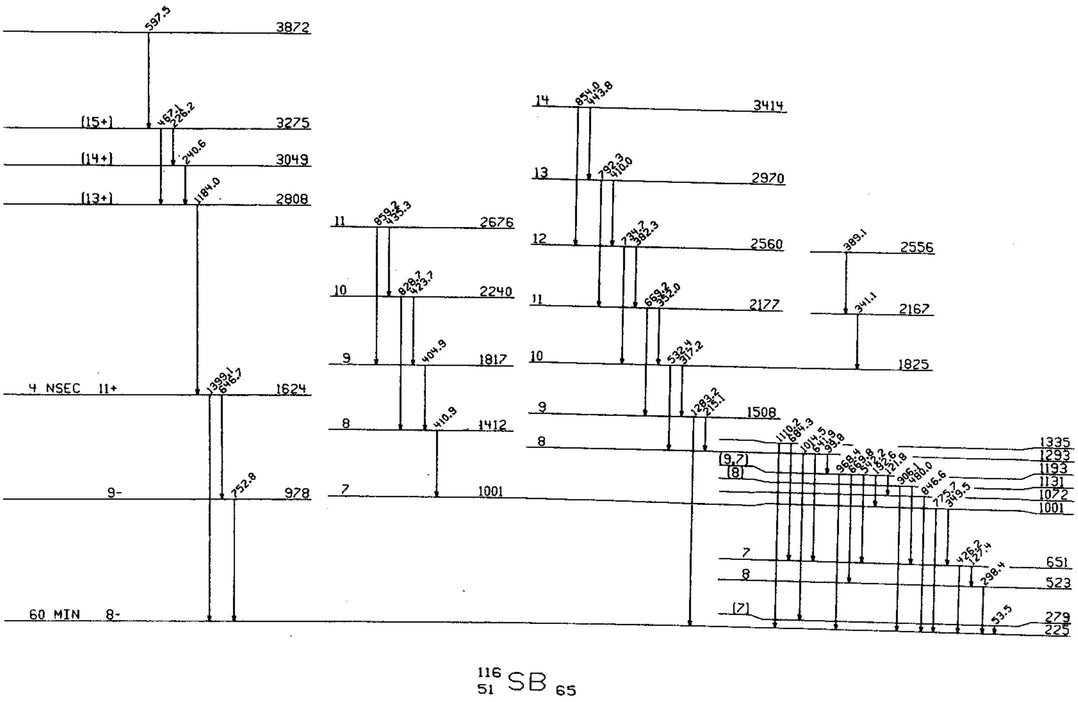

Fig. 1. Partial level scheme for ^{116}Sb showing those states populated in the ^{115}In(α,3nγ) reaction.

A plot of $\Delta E/2I$ vs $2I^2$ for these bands is shown in Fig. 2. ALso included in the figure are results from a study of ^{118}Sb, showing the same rotational bands. The similarity in the rotational structure of these two nuclei is immediatley obvious.

In conclusion the high spin structure of ^{116}Sb exhibits a variety of phenomena, closely related to the odd-mass Sb nuclei. Perhaps the most interesting of these is the existance of rotational bands built on deformed high spin states.

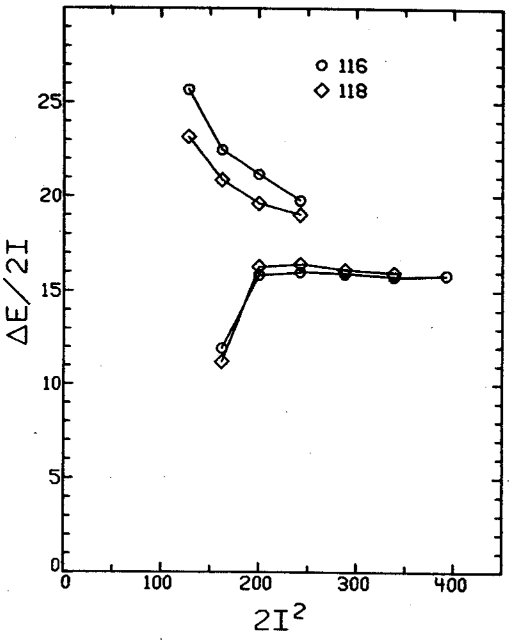

Fig. 2. The rotational band spacing as a function of I^2 for the bands in ^{116,118}Sb.

---

1. W.H. Bentley and W.H. Kelly, Annual Report 1977-1978 Cyclotron Laboratory, Michigan State University. 44
2. R. Kamermans, H.W. Jongsma, T.J. Ketel, R. Van Der Wey and H. Verheul, Nuclear Physics A266 (1976) 346.
3. C. Ekstrom, W. Hogervorst, S. Ingelman and G. Wannberg, Nuclear Physics S226 (1974) 219.
4. R.E. Shroy, A.K. Gaigalas, G. Schatz and D.B. Fossan, Phys. Rev. C 19 (1979) 1324.

Resolution of the ^{145}Gd ε/β^+ Decay Branching Ratio Anomalies

R.B. Firestone, R.C. Pardo, and Wm. C. McHarris

For several years we have been investigating apparently large anomalies in the ε/β^+ decay branching ratios from ^{145}Gd decay to several daughter levels in ^{145}Eu.[1,2] Repeated measurements with increasingly greater precision indicated that these anomalies must be correct unless a substantial discrepancy existed in the decay scheme. In 1976 we recorded a new γ-ray singles spectrum for ^{145}Gd decay with markedly improved statistics using a large volume Ge(Li) detector. In this spectrum we observed over 100 new γ-rays above 2.5 MeV which were not placed in the level scheme. These new transitions represented less than 4% of the total decay and could only account for a small fraction of the total observed anomalies. Later, Hardy et al.[3] suggested that due to the high level density above 2.5 MeV in ^{145}Eu there should be a large amount of electron capture decay to a continuum of unobserved states. Thus, the apparent excess of ε decay to some levels could result from actual feeding to higher lying levels which deexcite, unobserved, through theselower levels. In 1977 Hornshφj et al.[4] presented data which purported to substantiate Hardy's suggestion. In a γ-ray singles spectrum they found that 16% of the decay resulted from 250 γ-rays above 2.5 MeV and they extracted, from the γ-ray endpoint, a Q_ε which was 300 keV lower than the previously accepted value. These results were then reported to be sufficient, in principle, to explain the entire anomaly. It was further claimed that the decay scheme is too complicated to be experimentally elucidated.

We took exception to these results for several reasons. First the claim that 16% of all decay is in γ-rays above 2.5 MeV cnanot be reconciled with our data even if Compton background were included in the photopeak intensity. Second, the method of extracting the Q_ε value from γ-ray endpoints is at best dubious and is not acceptable within the limits of accuracy claimed by the authors because the spectrum is dominated by Compton events and the inevitable clustering of γ-ray intensity due to underlying nucleuar structure. In light of the clear improtance of knowing the decay scheme better, we decided to ignore Hornshφj et al.'s dire warning and work out the decay in a more orthodox fashion with improved statistics.

In order to convincingly unravel the true ^{145}Gd decay scheme we took several steps. First, an extremely high-statistics γ-ray singles spectrum was recorded containing 2×10^9 events. This spectrum yielded about 150 γ-rays above 2.5 MeV representing less than 6% of the total decay. Second we measured the Q_ε by the conventional β-γ coincidence technique. This result was described in last years annual report where we showed that the Q_ε was, indeed, 240 keV lower than previously assumed. Although this value agrees with that of Hornshφj et al., repetition of their method with our higher statistics gives a result 200 keV lower yet. Finally we obtained γ-γ coincidence data representing 10 times as much data as we previously used to generate the ^{145}Gd decay scheme. These data have been tediously analyzed to yield a new decay scheme with 336 γ-rays and 127 levels. Many new, important γ-ray transitions below 2.5 MeV were found which were masked in the γ-ray singles spectrum by the high background in this region but could be identified clearly in coincidence. The new transitions fed strongly those levels with the greatest anomalies. Our final decay scheme, broken down to six parts for convenience, is shown in figures 1a - 1f. The resulting ε/β^+ branching ratios are presented in Table I. There are no longer any large anomalies, and it is interesting to note that those levels thought to be most anomalous have virtually no remaining beta feeding.

---

1. R.B. Firestone, R.A. Warner, Wm. C. McHarris and W.H. Kelly, Phys. Rev. Lett. 33, 30 (1974).
2. R.B. Firestone, R.A. Warner, Wm. C. McHarris, and W.H. Kelly, Phys. Rev. Lett. 35, 401 (1975).
3. J.C. Hardy, L.C. Carraz, B. Jonson, and P.G. Hansen, Phys. Lett. 71B, 307 (1977).
4. P. Hornshφj, H.L. Nielsen, and N. Rud, Phys. Rev. Lett. 39, 537 (1977).

Table II. Absolute ε/β^+ Decay Branching Ratios for ^{145}Gd

Levels in ^{145}Eu	ε/β^+ Ratio		Skew Ratio (exp/theor)	Total % Feedings	
	Experiment	Calculated[a]		Coincidence[c]	Singles
808.5	b	0.56±0.03	b	1.89±0.92	0.61±0.67
1041.9	0.91±0.14	0.71±0.04	1.3±0.3	6.90±0.51	7.85±0.59
1567.3	<143	1.26±0.09	<143	0.74±0.25	0.65±0.07
1599.9	b	1.31±0.10	b	0.37±0.31	0.18±0.14
1757.8	1.93±0.20	1.62±0.13	1.2±0.2	≡33.40±2.05	33.40±1.93
1761.9	2.9 ±1.3	1.62±0.14	1.8±1.0	1.17±0.33	1.25±0.10
1845.4	<191	1.82±0.15	<191	0.22±0.21	0.13±0.05
1880.6	2.14±0.20	1.92±0.15	11.1±0.2	30.92±1.74	34.16±1.83
2048.9	3.8 ±1.9	2.47±0.25	1.5±0.9	0.84±0.24	0.91±0.08
2113.9	13 ±6	2.75±0.27	<18	0.65±0.19	0.32±0.03
2494.8	5.2 ±1.4	5.4 ±0.7	1.0±0.4	1.24±0.23	1.41±0.07
2642.2	8.0 ±1.8	7.6 ±1.2	11.1±0.4	2.15±0.34	2.18±0.12

---

[a] N.B. Gove and M.J. Martin, Nucl. Data Tables 10, 205 (1971). Calculated from $Q_\varepsilon = 5.07\pm0.06$ MeV.

[b] Indeterminate from the data. No significant direct β feeding remains after correction for feeding from higher lying states.

[c] Inferred from coincidence intensity balances.

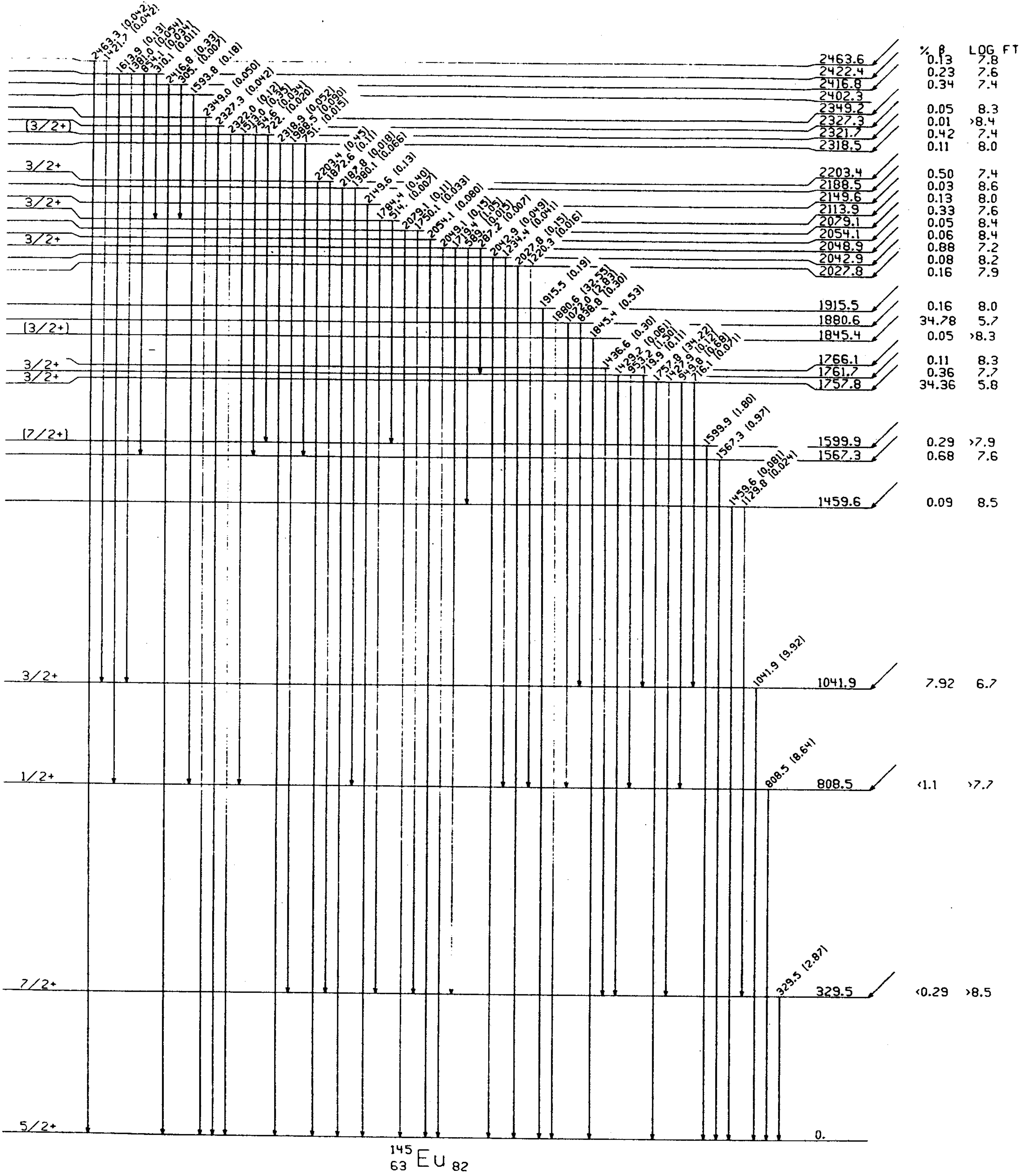
% β
LOG FT
2463.6 0.13 7.8
2422.4 0.23 7.6
2416.8 0.34 7.4
2402.3
2349.2 0.05 8.3
2327.3 0.01 >8.4
2321.7 0.42 7.4
2318.5 0.11 8.0
2203.4 0.50 7.4
2188.5 0.03 8.6
2149.6 0.13 8.0
2113.9 0.33 7.6
2079.1 0.05 8.4
2054.1 0.06 8.4
2048.9 0.88 7.2
2042.9 0.08 8.2
2027.8 0.16 7.9
1915.5 0.16 8.0
1880.6 34.78 5.7
1845.4 0.05 >8.3
1766.1 0.11 8.3
1761.7 0.36 7.7
1757.8 34.36 5.8
1599.9 0.29 >7.9
1567.3 0.68 7.6
1459.6 0.09 8.5
1041.9 7.92 6.7
808.5 <1.1 >7.7
329.5 <0.29 >8.5
0.
(3/2+)
3/2+
3/2+
3/2+
(3/2+)
3/2+
3/2+
(7/2+)
3/2+
1/2+
7/2+
5/2+
2463.3 (0.042)
1421.7 (0.042)
1613.9 (0.13)
1381.0 (0.054)
854.1 (0.034)
310.1 (0.011)
2416.8 (0.33)
305. (0.007)
1593.8 (0.18)
2349.0 (0.050)
2327.3 (0.042)
2322.0 (0.12)
1513.0 (0.35)
754.6 (0.034)
722. (0.020)
2318.9 (0.052)
1988.5 (0.090)
751. (0.015)
2203.4 (0.45)
1872.6 (0.11)
2187.8 (0.018)
1380.1 (0.066)
2149.6 (0.13)
1784.4 (0.40)
514. (0.007)
2079.1 (0.11)
1750.1 (0.033)
2054.1 (0.080)
2049.1 (0.15)
1719.4 (1.05)
589. (0.015)
287.2 (0.007)
2042.9 (0.049)
1234.4 (0.041)
2027.8 (0.15)
1220.3 (0.016)
1915.5 (0.19)
1880.6 (32.55)
1072.0 (2.83)
838.8 (0.30)
1845.4 (0.53)
1436.6 (0.30)
1429.2 (0.061)
953.2 (1.50)
719.9 (0.11)
1757.8 (34.22)
1427.9 (0.12)
949.8 (0.68)
716.1 (0.071)
1599.9 (1.80)
1567.3 (0.97)
1459.6 (0.081)
1129.8 (0.024)
1041.9 (9.92)
808.5 (8.64)
329.5 (2.87)
$^{145}_{63}\mathrm{Eu}_{82}$

Fig. 1a

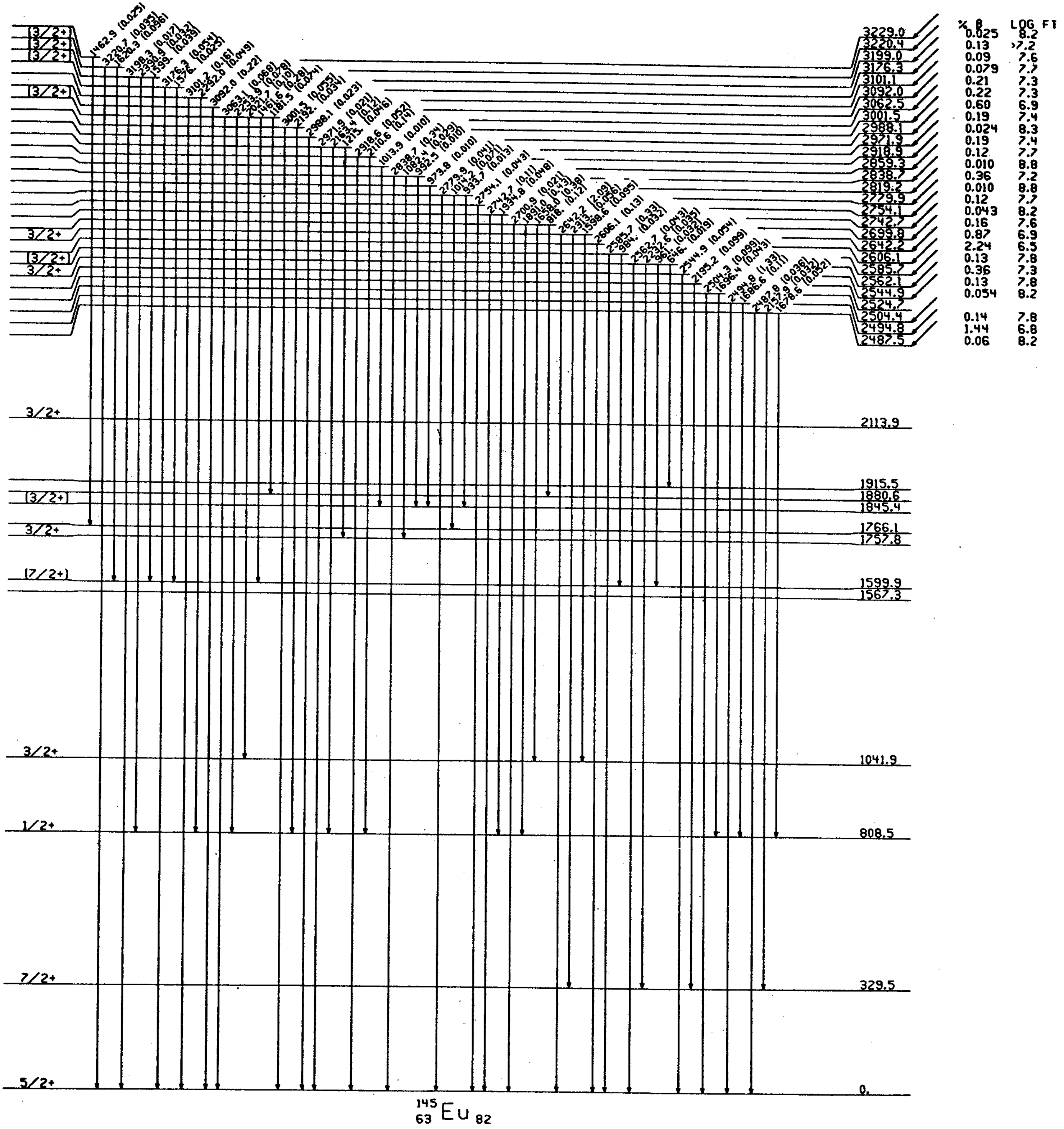
% β
LOG FT
3229.0 0.025 8.2
3220.4 0.13 >7.2
3199.0 0.09 7.6
3176.3 0.079 7.7
3101.1 0.21 7.3
3092.0 0.22 7.3
3062.5 0.60 6.9
3001.5 0.19 7.4
2988.1 0.024 8.3
2971.9 0.19 7.4
2918.9 0.12 7.7
2859.3 0.010 8.8
2838.7 0.36 7.2
2819.2 0.010 8.8
2779.9 0.12 7.7
2754.1 0.043 8.2
2742.7 0.16 7.6
2699.8 0.87 6.9
2642.2 2.24 6.5
2606.1 0.13 7.8
2585.7 0.36 7.3
2562.1 0.13 7.8
2544.9 0.054 8.2
2524.7
2504.4 0.14 7.8
2494.8 1.44 6.8
2487.5 0.06 8.2
(3/2+)
(3/2+)
(3/2+)
(3/2+)
3/2+
(3/2+)
3/2+
1462.9 (0.025)
3220.7 (0.035)
1620.3 (0.096)
3198.3 (0.017)
2390.9 (0.032)
1599. (0.039)
3176.3 (0.054)
1576. (0.025)
3101.2 (0.16)
2292.0 (0.049)
3092.0 (0.22)
3063.1 (0.068)
2253.9 (0.078)
2021.7 (0.10)
1461.6 (0.28)
1181.5 (0.074)
3001.5 (0.055)
2192. (0.034)
2988.1 (0.023)
2971.9 (0.021)
2163.4 (0.12)
1215. (0.046)
2918.6 (0.052)
2110.6 (0.14)
1013.9 (0.010)
2838.7 (0.34)
1082.4 (0.029)
992.5 (0.010)
973.8 (0.010)
2779.9 (0.041)
1014.2 (0.071)
933.7 (0.013)
2754.1 (0.043)
2742.7 (0.11)
1934.8 (0.048)
2700.9 (0.021)
1891.0 (0.43)
1658.0 (0.38)
818. (0.12)
2642.2 (2.09)
2313. (0.056)
1598.6 (0.095)
2606.1 (0.13)
2585.7 (0.33)
984. (0.032)
2562.7 (0.043)
2232.6 (0.035)
961. (0.032)
646. (0.019)
2544.9 (0.054)
2195.2 (0.099)
2504.3 (0.099)
1696.4 (0.043)
2494.8 (1.33)
1686.6 (0.11)
2487.8 (0.036)
2157.9 (0.032)
1678.6 (0.052)
3/2+ 2113.9
1915.5
(3/2+) 1880.6
1845.4
3/2+ 1766.1
1757.8
(7/2+) 1599.9
1567.3
3/2+ 1041.9
1/2+ 808.5
7/2+ 329.5
5/2+ 0.
$^{145}_{63}$Eu$_{82}$

Fig. 1b

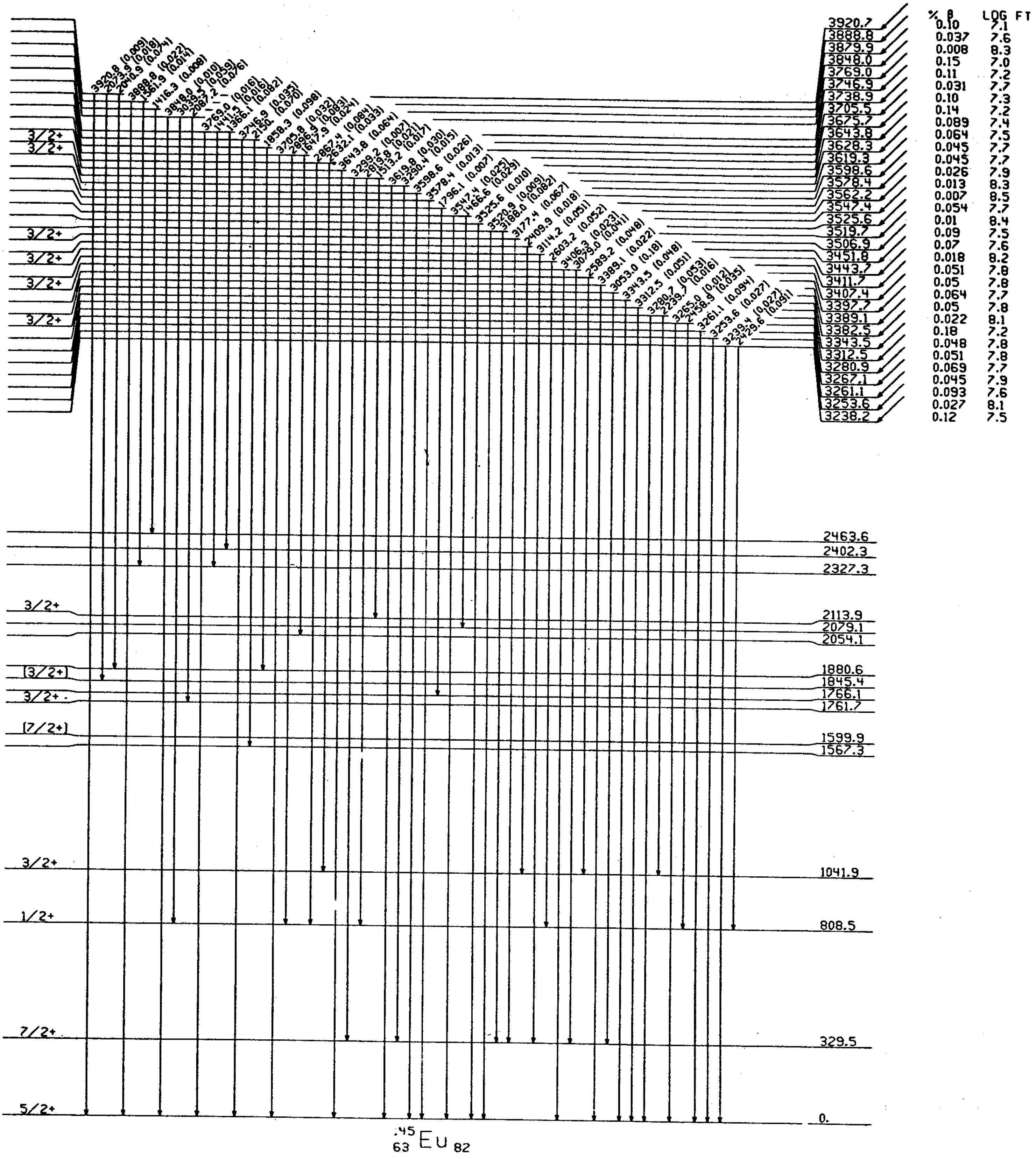
% β
LOG FT
3920.7 0.10 7.1
3888.8 0.037 7.6
3879.9 0.008 8.3
3848.0 0.15 7.0
3769.0 0.11 7.2
3746.9 0.031 7.7
3738.9 0.10 7.3
3705.5 0.14 7.2
3675.7 0.089 7.4
3643.8 0.064 7.5
3628.3 0.045 7.7
3619.3 0.045 7.7
3598.6 0.026 7.9
3578.4 0.013 8.3
3562.2 0.007 8.5
3547.4 0.054 7.7
3525.6 0.01 8.4
3519.7 0.09 7.5
3506.9 0.07 7.6
3451.8 0.018 8.2
3443.7 0.051 7.8
3411.7 0.05 7.8
3407.4 0.064 7.7
3397.7 0.05 7.8
3389.1 0.022 8.1
3382.5 0.18 7.2
3343.5 0.048 7.8
3312.5 0.051 7.8
3280.9 0.069 7.7
3267.1 0.045 7.9
3261.1 0.093 7.6
3253.6 0.027 8.1
3238.2 0.12 7.5
3920.8 (0.009)
2073.9 (0.018)
2040.9 (0.074)
3888.8 (0.022)
1561.9 (0.014)
1416.3 (0.008)
3848.0 (0.010)
3039.5 (0.059)
2087.2 (0.076)
3769.0 (0.016)
1441.5 (0.016)
1966.1 (0.070)
3746.9 (0.082)
2150. (0.035)
1858.3 (0.098)
3705.8 (0.032)
2896.9 (0.083)
1647.9 (0.024)
2867.4 (0.084)
2632.1 (0.033)
3643.8 (0.064)
3299.2 (0.007)
2819.8 (0.021)
1513.2 (0.017)
3619.8 (0.030)
3290.4 (0.015)
3598.6 (0.026)
3578.4 (0.013)
1796.1 (0.007)
3547.4 (0.025)
1466.6 (0.029)
3525.6 (0.010)
3520.9 (0.009)
3188.0 (0.082)
3177.4 (0.067)
2409.9 (0.018)
3114.2 (0.051)
2603.2 (0.052)
3406.3 (0.023)
3079.0 (0.041)
2589.2 (0.048)
3389.1 (0.022)
3053.0 (0.18)
3343.5 (0.048)
3312.5 (0.051)
3280.7 (0.053)
2239.7 (0.016)
3265.0 (0.012)
2458.9 (0.035)
3261.1 (0.094)
3253.6 (0.027)
3239.4 (0.027)
2429.6 (0.091)
3/2+
3/2+
3/2+
3/2+
3/2+
3/2+
2463.6
2402.3
2327.3
3/2+
2113.9
2079.1
2054.1
[3/2+]
1880.6
1845.4
3/2+
1766.1
1761.7
[7/2+]
1599.9
1567.3
3/2+
1041.9
1/2+
808.5
7/2+
329.5
5/2+
0.
$^{145}_{63}\mathrm{Eu}_{82}$

Fig. 1c

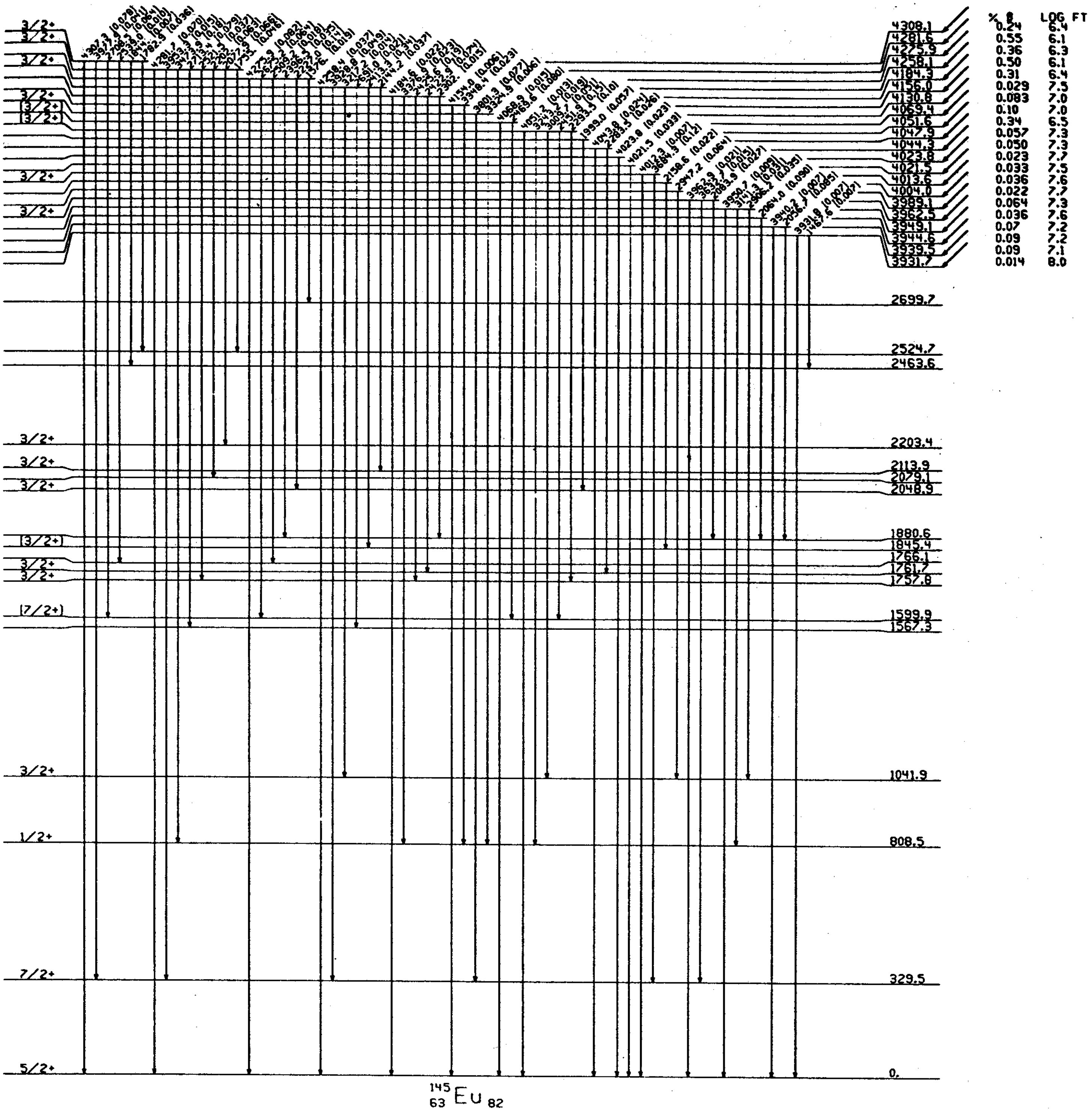
3/2+
3/2+
3/2+
3/2+
(3/2+)
(3/2+)
3/2+
3/2+
4307.3 (0.078)
3978.6 (0.011)
2708.5 (0.064)
2539.0 (0.010)
1844.5 (0.007)
1782.9 (0.036)
4281.7 (0.070)
3953.3 (0.015)
3473.9 (0.18)
2713.4 (0.079)
2521.5 (0.037)
2202.7 (0.063)
2077.9 (0.066)
1757. (0.046)
4275.9 (0.082)
2675.2 (0.064)
2509.2 (0.018)
2396.3 (0.035)
2227.0 (0.14)
1576. (0.019)
4258.4 (0.037)
3928.8 (0.049)
3217.2 (0.014)
2691.0 (0.021)
2413.3 (0.34)
2144.2 (0.037)
4184.6 (0.022)
3376.9 (0.023)
2423.6 (0.19)
2422.9 (0.074)
2302. (0.015)
4154.0 (0.006)
3348.4 (0.023)
3801.3 (0.027)
3324.9 (0.006)
4068.9 (0.015)
2469.6 (0.080)
4051.2 (0.013)
3243.2 (0.019)
3009.7 (0.031)
2451.9 (0.15)
2293.5 (0.10)
1999.0 (0.057)
4043.8 (0.024)
2283.5 (0.026)
4023.8 (0.023)
4021.5 (0.033)
4012.3 (0.007)
3684.3 (0.12)
2158.6 (0.022)
2947.2 (0.064)
3962.9 (0.021)
3632.7 (0.015)
2083.9 (0.027)
3950.7 (0.009)
3141.3 (0.031)
2906.2 (0.035)
2064.0 (0.090)
3940.2 (0.007)
2056.7 (0.085)
3931.8 (0.007)
1467.6 (0.007)
4308.1
4281.6
4275.9
4258.1
4184.3
4156.0
4130.8
4069.4
4051.6
4047.9
4044.3
4023.8
4021.5
4013.6
4004.0
3989.1
3962.5
3949.1
3944.6
3939.5
3931.7
% β LOG FT
0.24 6.4
0.55 6.1
0.36 6.3
0.50 6.1
0.31 6.4
0.029 7.5
0.083 7.0
0.10 7.0
0.34 6.5
0.057 7.3
0.050 7.3
0.023 7.7
0.033 7.5
0.036 7.6
0.022 7.7
0.064 7.3
0.036 7.6
0.07 7.2
0.09 7.2
0.09 7.1
0.014 8.0
2699.7
2524.7
2463.6
3/2+ 2203.4
3/2+ 2113.9
2079.1
3/2+ 2048.9
(3/2+) 1880.6
1845.4
3/2+ 1766.1
3/2+ 1761.7
1757.8
(7/2+) 1599.9
1567.3
3/2+ 1041.9
1/2+ 808.5
7/2+ 329.5
5/2+ 0.
145 63 Eu 82

Fig. 1d

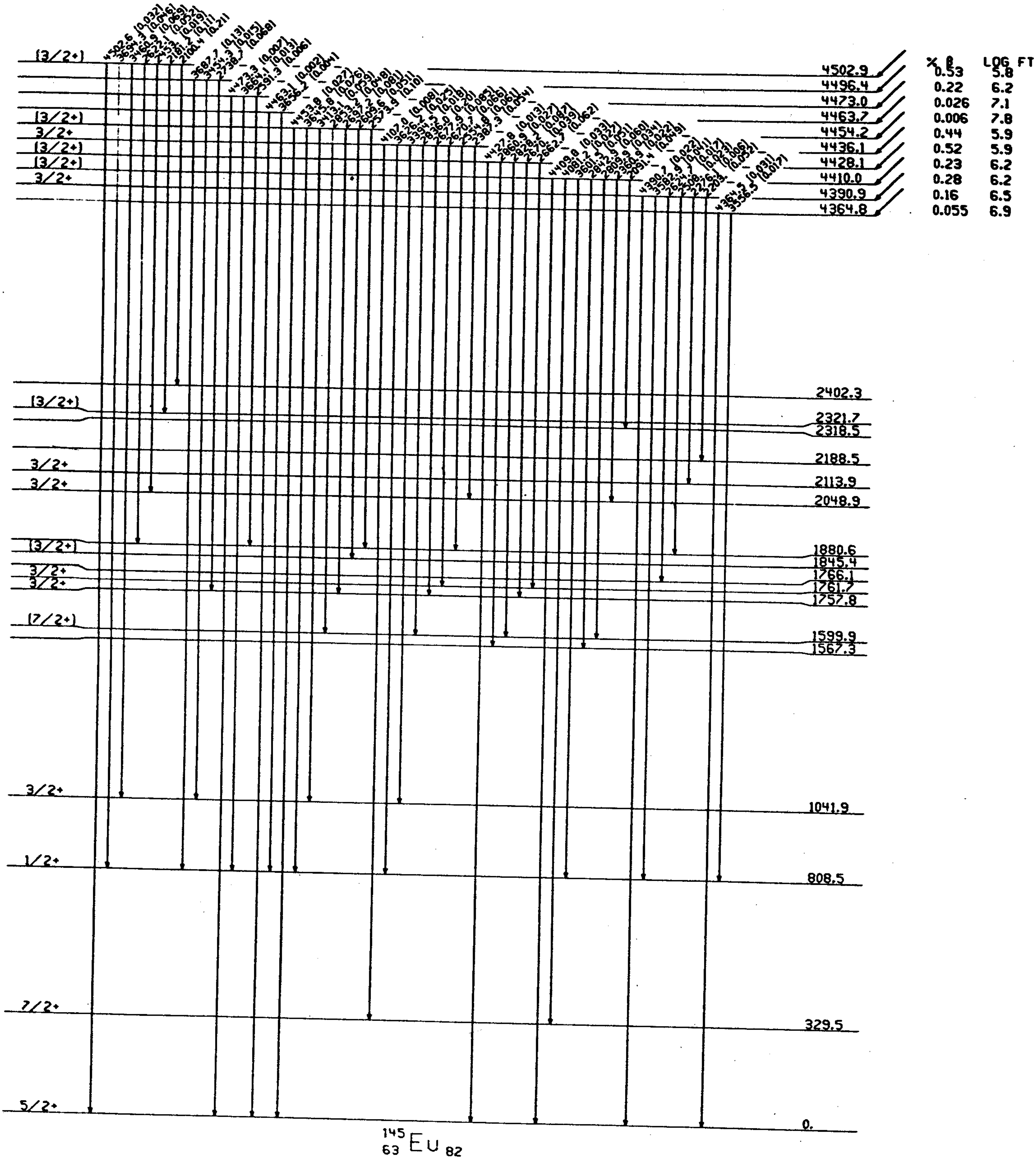
(3/2+)
(3/2+)
3/2+
(3/2+)
(3/2+)
3/2+
4502.6 (0.032)
3694.3 (0.046)
3460.9 (0.069)
2622.1 (0.052)
2315.3 (0.019)
2181.2 (0.11)
2100.4 (0.21)
3687.7 (0.13)
3454.3 (0.015)
2738.7 (0.068)
4473.3 (0.007)
3664.1 (0.013)
2591.3 (0.006)
4463.1 (0.002)
3656.2 (0.004)
4453.8 (0.027)
3645.8 (0.076)
3413.1 (0.059)
2853.3 (0.048)
2697.2 (0.081)
2609.6 (0.051)
2573.9 (0.10)
4107.0 (0.008)
3626.2 (0.025)
3394.5 (0.018)
2836.0 (0.20)
2677.9 (0.085)
2670.7 (0.066)
2554.8 (0.061)
2387.3 (0.054)
4427.8 (0.013)
2860.9 (0.027)
2828.2 (0.087)
2670. (0.039)
2662.7 (0.062)
4409.8 (0.033)
4081.2 (0.027)
3601.5 (0.051)
2842.9 (0.060)
2809.9 (0.034)
2360.9 (0.022)
2091.4 (0.049)
4390.7 (0.022)
3582.9 (0.041)
2624.7 (0.017)
2508. (0.023)
2276.1 (0.006)
2203. (0.032)
4364.5 (0.031)
3556.5 (0.017)
% β
LOG FT
4502.9
0.53
5.8
4496.4
0.22
6.2
4473.0
0.026
7.1
4463.7
0.006
7.8
4454.2
0.44
5.9
4436.1
0.52
5.9
4428.1
0.23
6.2
4410.0
0.28
6.2
4390.9
0.16
6.5
4364.8
0.055
6.9
2402.3
(3/2+)
2321.7
2318.5
3/2+
2188.5
3/2+
2113.9
2048.9
(3/2+)
1880.6
1845.4
3/2+
1766.1
3/2+
1761.7
1757.8
(7/2+)
1599.9
1567.3
3/2+
1041.9
1/2+
808.5
7/2+
329.5
5/2+
0.
$^{145}_{63}$Eu$_{82}$

Fig. 1e

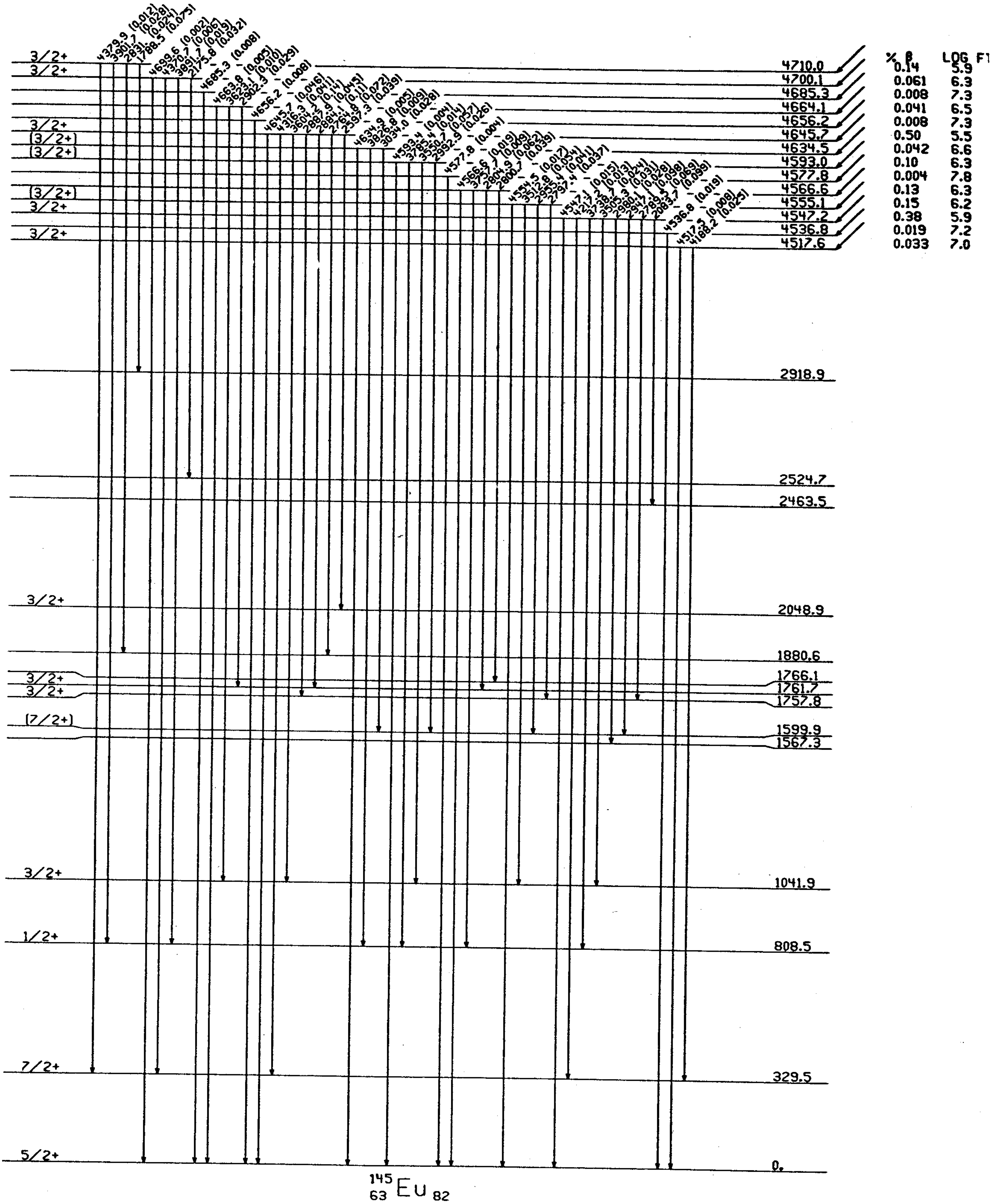
4379.9 (0.012)
3901.7 (0.028)
2831. (0.024)
1788.5 (0.075)
4699.6 (0.002)
4370.7 (0.006)
3891.7 (0.019)
2175.8 (0.032)
4685.3 (0.008)
4663.8 (0.005)
3623.1 (0.010)
2902.3 (0.029)
4656.2 (0.008)
4645.7 (0.046)
4316.3 (0.041)
3604.2 (0.14)
2887.9 (0.045)
2884.1 (0.11)
2764.8 (0.072)
2597.3 (0.039)
4634.9 (0.005)
3826.8 (0.009)
3034.0 (0.028)
4593.4 (0.004)
3785.4 (0.014)
3550.7 (0.057)
2992.9 (0.026)
4577.8 (0.004)
4566.6 (0.019)
3757.7 (0.009)
2804.9 (0.062)
2800.7 (0.039)
4554.5 (0.012)
3512.8 (0.054)
2955.4 (0.041)
2797.4 (0.037)
4547.1 (0.015)
4217.2 (0.013)
3738.7 (0.024)
3505.3 (0.031)
2980.1 (0.028)
2947.1 (0.098)
2789.5 (0.069)
2083.7 (0.099)
4536.8 (0.019)
4517.5 (0.008)
4188.2 (0.025)
% β
LOG FT
3/2+ 4710.0 0.14 5.9
3/2+ 4700.1 0.061 6.3
4685.3 0.008 7.3
4664.1 0.041 6.5
3/2+ 4656.2 0.008 7.3
(3/2+) 4645.7 0.50 5.5
(3/2+) 4634.5 0.042 6.6
4593.0 0.10 6.3
(3/2+) 4577.8 0.004 7.8
3/2+ 4566.6 0.13 6.3
4555.1 0.15 6.2
3/2+ 4547.2 0.38 5.9
4536.8 0.019 7.2
4517.6 0.033 7.0
2918.9
2524.7
2463.5
3/2+ 2048.9
1880.6
3/2+ 1766.1
3/2+ 1761.7
1757.8
(7/2+) 1599.9
1567.3
3/2+ 1041.9
1/2+ 808.5
7/2+ 329.5
5/2+ 0.
$^{145}_{63}$Eu$_{82}$

Fig. 1f

Measurement of the M1 Analogue γ-ray Transition to ^{22}Na Beta Decay

R.B. Firestone and L. Harwood

A large body of experimental data exists concerning the hindered allowed beta decay of ^{22}Na. In addition to the extremely accurate log ft value, precise measurements of the e/β^+ branching ratio and the β-γ directional correlation coefficient A_{22} deviate markedly from the prediction of allowed β-decay theory. Firestone and Holstein have shown that these deviations can be explained by the inclusion of four second order matrix elements into the theory.[1] Although most experimental beta decay parameters are dependent on a combination of these matrix elements, the weak magnetism form factor b/Ac is uniquely related to the transition probability of the analogue M1 γ-ray by CVC theory.

In ^{22}Na the analogue to the $T = 1$, 2^+ daughter state of ^{22}Ne is located at an excitation of 1952 keV. This state deexcites strongly to the $T = 0$, 1^+ state at 583 keV, and prior to this work the direct ground state analogue transition was not observed. In order to measure this transition probability we produced ^{22}Na by the ^{25}Mg$(p,\alpha)^{22}$Na reaction. This reaction strongly populated excited states which fed the 1952 keV level. α-γ coincidences were measured with a Si detector telescope to reduce (p,p') events and a large volume Ge(Li) detector. The resultant coincidence γ-ray spectrum is shown in Fig. 1 where the 1952-keV γ-ray is weakly observed with an intensity of 0.61 ± 0.27% per decay from the level. The half-life for this level has been measured[2] as 11 ± 3 fs yielding a radiative width of 3.6×10^{-4} ev. From this result the weak magnetism form factor b/Ac = 14 ± 6 can be calculated. This value is too small to explain the observed e/β^+ ratio and A_{22}, however, an additional measurement, such as the beta polarization, would allow the direct specification of all four second order matrix elements.

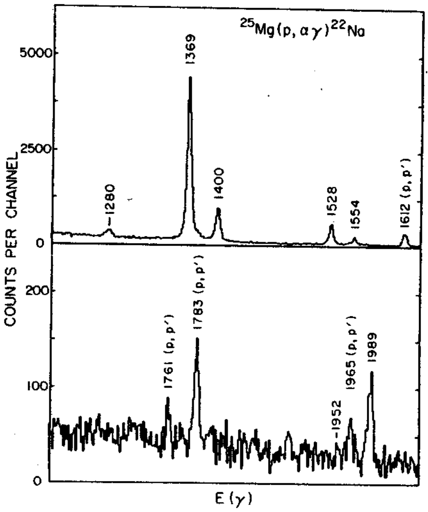

---

1. R.B. Firestone, Wm. C. McHarris, and B.R. Holstein, Phys. Rev. C18, 2719 (1978).
2. M. Bister, A. Anttila, and J. Keinonen, Nucl. Phys. A306, 189 (1978).

A Study of 6.13 MeV γ Rays from ^{16}O(p,p'γ)^{16}O

J. Narayanaswamy, S. Faber, Sam M. Austin, and W. Bentley

Cross sections for the reactions ^{16}O(p,p'γ)^{16}O and ^{16}O(p,p$\alpha\gamma$)^{12}C yielding 6.13 and 4.44 MeV γ rays, respectively, are astrophysically important. Laboratory studies of these reactions are required for interpretation of observations of these lines made with spectrometers mounted on balloons and satellites. With this motivation, we undertook a study of these reactions at lab proton energies of 23.8, 35.3 and 44.7 MeV, using a gaseous oxygen target.

We are currently extracting total cross sections from and looking at the detailed line shapes of the observed γ ray spectra. Here we report results of a preliminary reduction of the 23.8 MeV data.

The 6.13 MeV line arises from an E3 transition, and determination of the total cross section requires measurements at atleast 4 angles. A 16% Ge(Li) detector mounted on the gonimeter arm was used to observe λ rays at various angles. A 9% Ge(Li) detector fixed in space, was used as a monitor. The gas cell had a window made of 1 mil thick kapton. Measurements were made from 60° to 150° in steps of 15° with the cell gas filled (1 atmosphere oxygen) and with the cell empty. Background due to the cell was subtracted, using the ratio of effective charge (effective charge = incident charge X live time) as the normalization factor. This same factor was also used to normalize between different angles.

Typical spectra are shown in Fig. 1. Dead times were usually 15-20%. Detector resolution at 6.13 MeV was about 15 keV, but the peaks were much wider due to Doppler broadening. The absolute efficiency of the detector was measured at various energies using calibrated sources of ^{60}Co, ^{152}Eu, and ^{238}Pu + ^{13}C (giving 6.13 MeV γ rays). During one run we also prepared ^{66}Ga by bombarding zinc foil with protons. Measurements with this source gave relative efficiencies for the energy range 0.8 to 4.8 MeV.

Preliminary reduction of the 23.8 MeV data gave the following total cross section for the 6.13 meV line.

Peak Analyzed	σ_{total} (mb)
Full energy peak (F.E.P.)	72.0
Single escape peak (S.E.P.)	60.0
Double escape peak (D.E.P.)	57.5

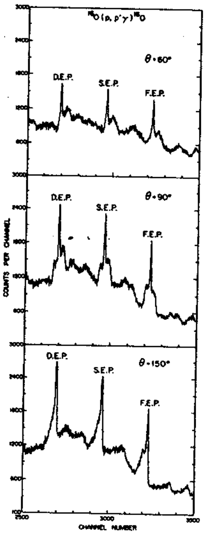

Figure 1

Due to Doppler broadening it is impssible to resolve the full energy peak at 6.13 MeV from the double escape peak of 7.1187 MeV γ rays. This explains the slightly higher value of σ_{total} obtained from the full energy peak analysis. At present our estimated error in $d\sigma/d\Omega$ is about 9% and in σ_{total} is about 20%. These preliminary results compare favorably with that of Dyer et al.[1] who obtain σ_{total} ~55 mb at about 23.8 MeV lab proton energy.

---

1. P. Dyer and D. Bodansky, private communication.